

Counterion displacement assay with Biginelli product: Ratiometric Sensor for Hg²⁺ and Resultant complex as sensor for Cl⁻

AmanpreetKaur,^a HemantSharma,^b NarinderSingh,^b NavneetKaur^{a*}

^a Centre for Nanoscience and Nanotechnology (UIEAST), Panjab University, Chandigarh, India, 160014.

^bDepartment of Chemistry, Indian Institute of Technology Ropar (IIT Ropar), Rupnagar, Panjab, India, 140001.

Corresponding Author: + 911722534464
navneetkaur@pu.ac.in

Table of Contents

Figure S1. ¹H NMR spectrum of Sensor1.

Figure S2. ¹³C NMR spectrum of Sensor1.

Figure S3. IR spectrum of Sensor1.

Figure S4. Mass spectrum of Sensor1.

Figure S5. ¹H NMR spectrum of Sensor2.

Figure S6. ¹³C NMR spectrum of Sensor2.

Figure S7. IR spectrum of Sensor2.

Figure S8. Mass spectrum of Sensor2.

Figure S9. Partial ¹H NMR spectrum of Sensor1 + Hg²⁺.

Figure S10. Partial IR spectrum of Sensor1 and 1 + Hg²⁺.

Figure S11. UV-Vis absorption spectra of 1-2 (10 μM) in DMF/H₂O (7/3; v/v) solvent system.

Figure S12. Fluorescence spectra of 1-2 (10 μM) in DMF/H₂O (7/3; v/v) solvent system (λ_{ex}=338 nm).

Figure S13. Salt perturbation studies of 1 recorded with 10 μM concentration of sensor in DMF/H₂O (7:3, v/v) solvent system with the respective fluorescence spectrum recorded upon addition of 100 equiv. of tetrabutylammonium nitrate under the same concentration of sensor and solvent system.

Figure S14. Job's plot between sensor1 and Hg(II). The concentration of [HG] was calculated by the equation [HG] = ΔI/I₀ × [H].

Figure S15. pH titration of Sensor **1** (10 μM) in DMF/H₂O (1/9; v/v) solvent system (λ_{ex} =338 nm).

Figure S16. UV-Vis absorption spectra of (**1**)₂.Hg²⁺ (2.5 μM) in THF/H₂O (4:1, v/v) solvent system.

Figure S17. Fluorescence spectrum of (**1**)₂.Hg²⁺ (2.5 μM) in THF/H₂O (4:1, v/v) solvent system (λ_{ex} =338 nm).

Figure S18. Size distribution of complex (**1**)₂.Hg²⁺ in DMF/H₂O (8:92, v/v) solvent system.

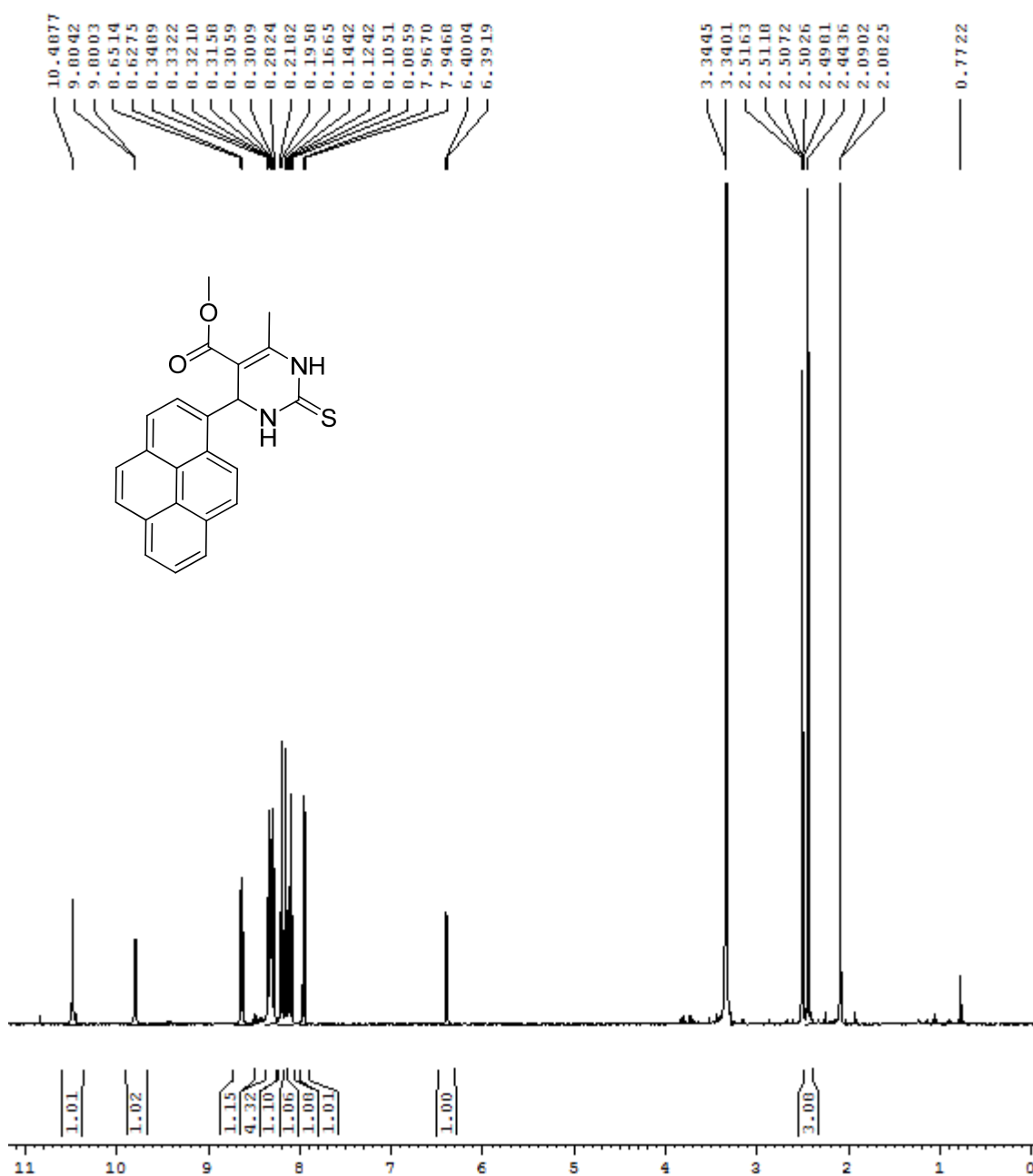


Figure S1. ^1H NMR spectrum of Sensor1.

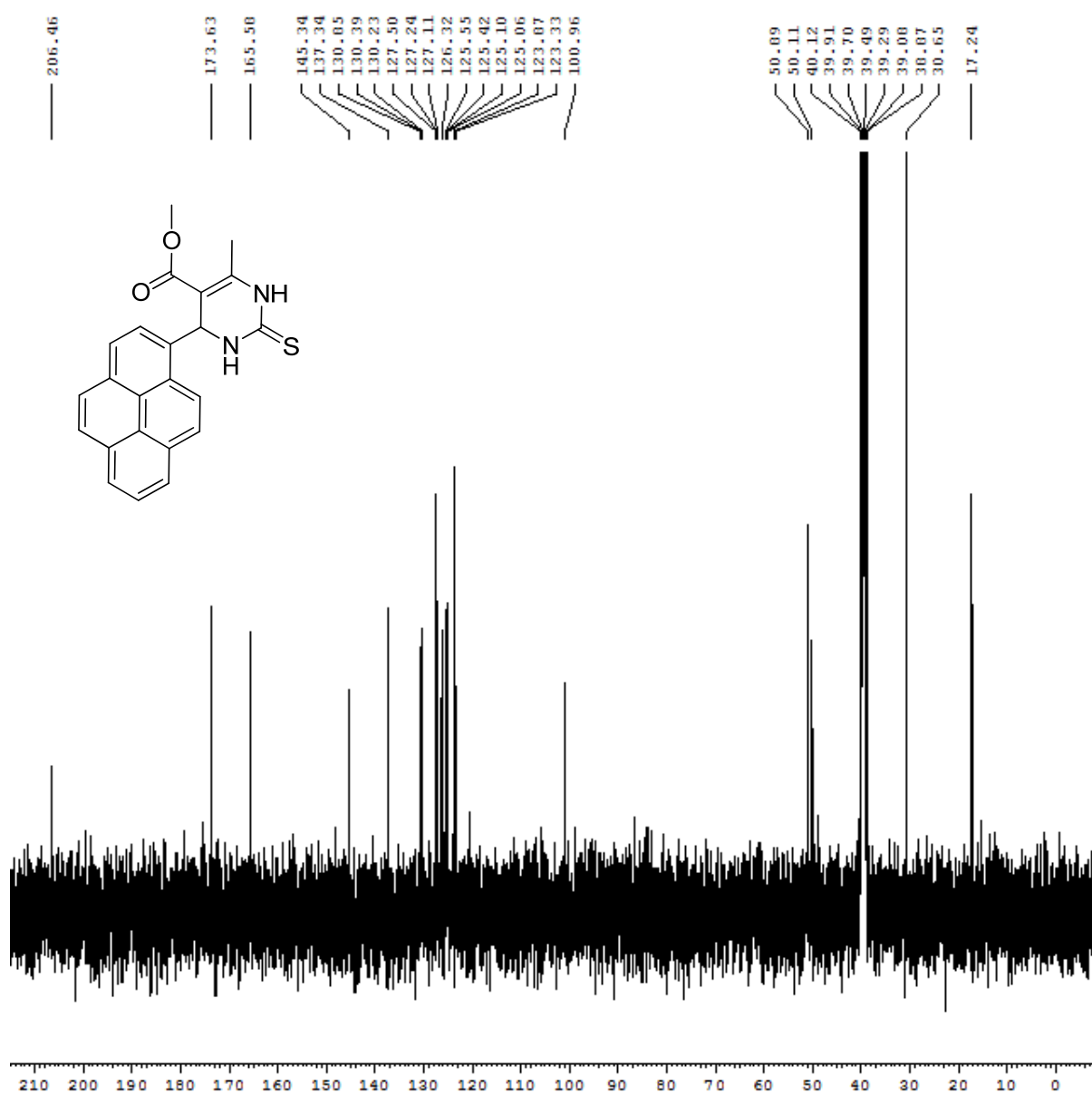


Figure S2. ^{13}C NMR spectrum of Sensor1.

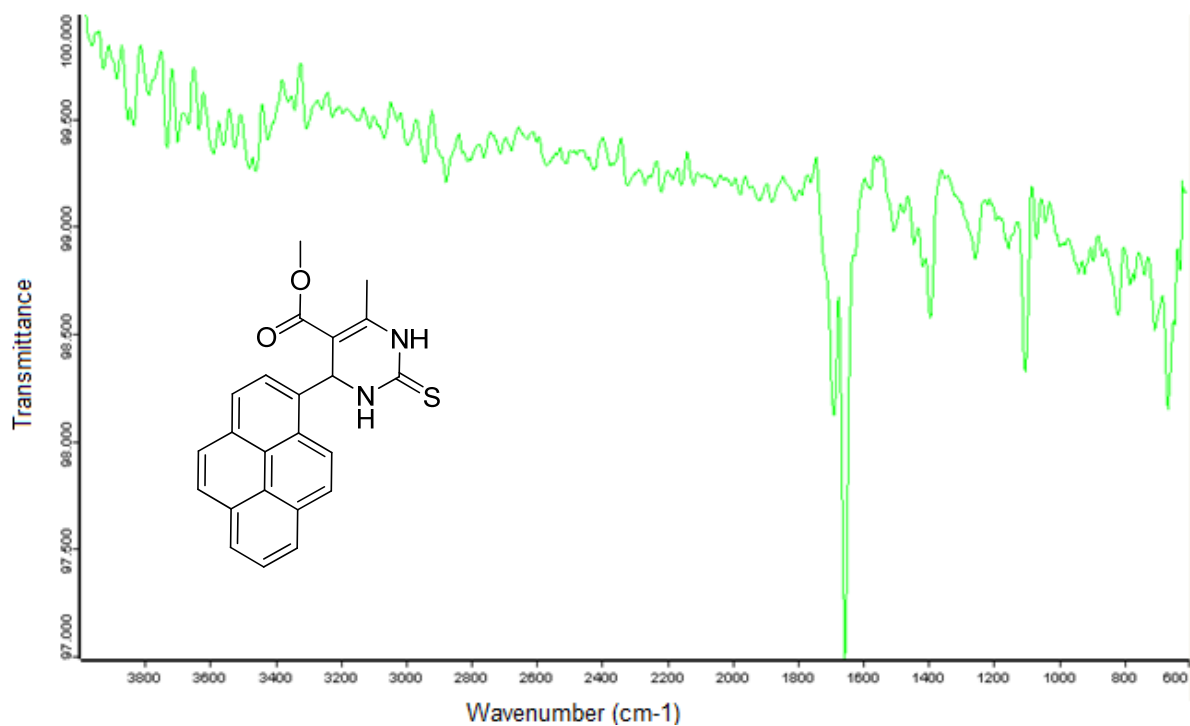


Figure S3. IR spectrum of Sensor1.

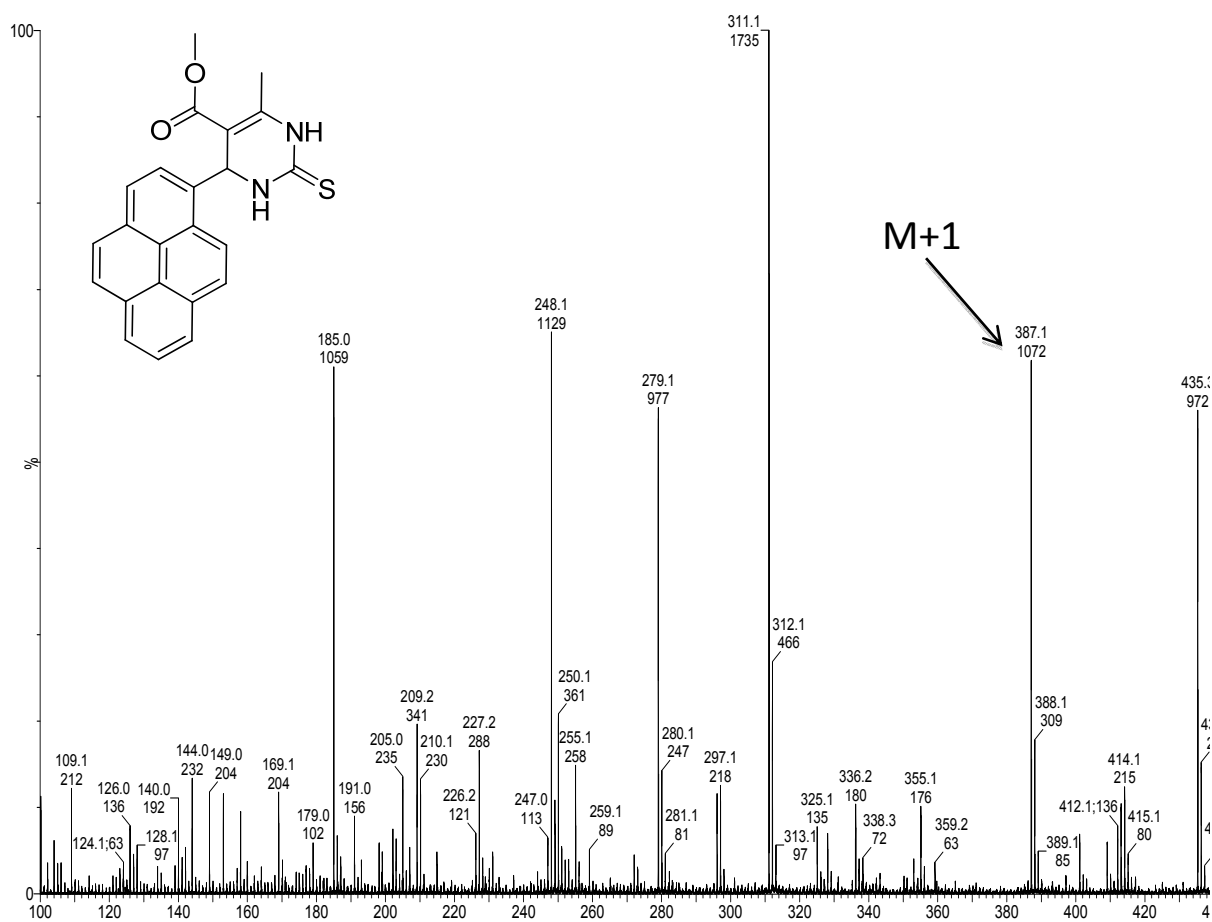


Figure S4. Mass spectrum of Sensor1.

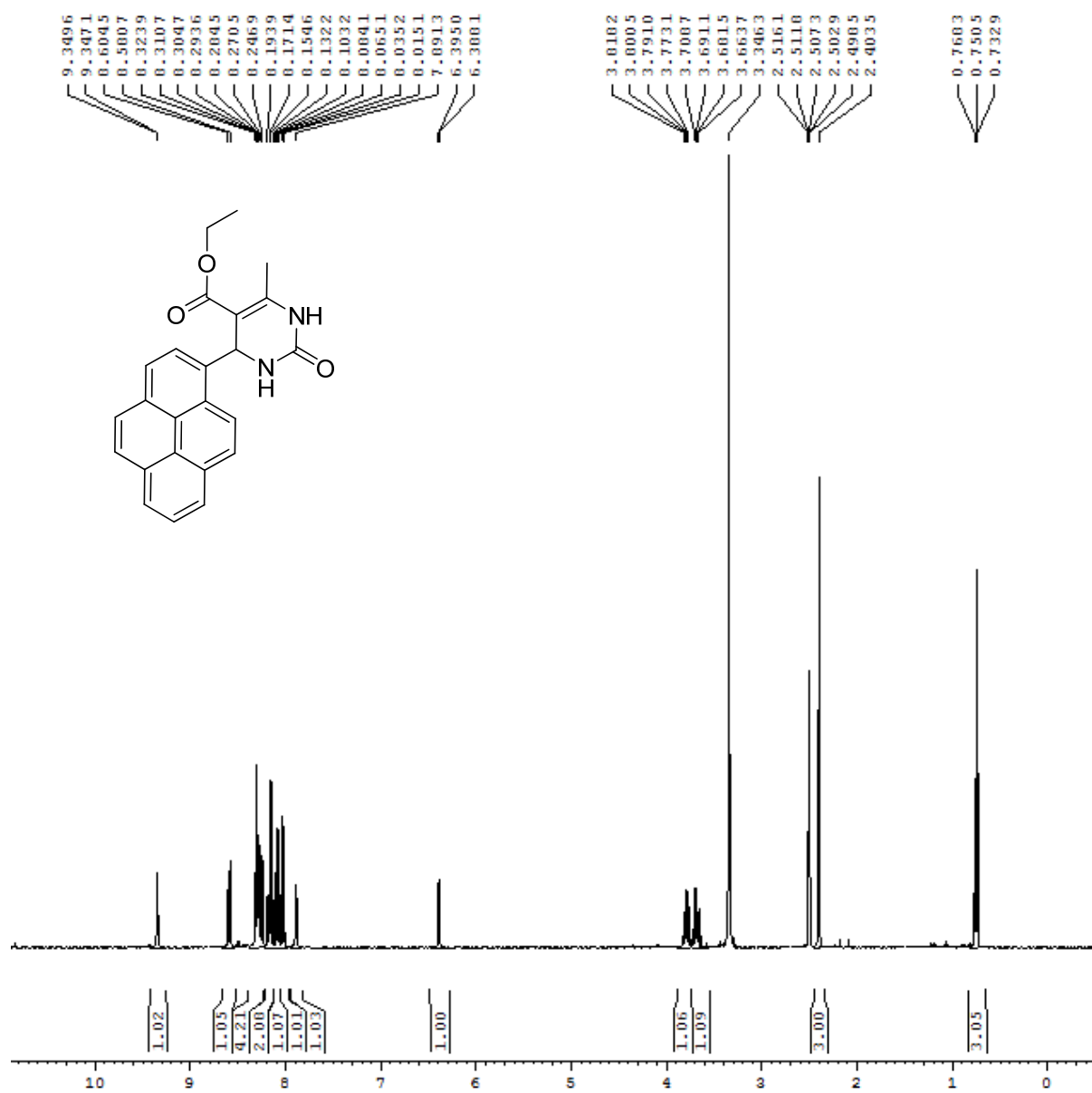


Figure S5. ¹H NMR spectrum of Sensor2.

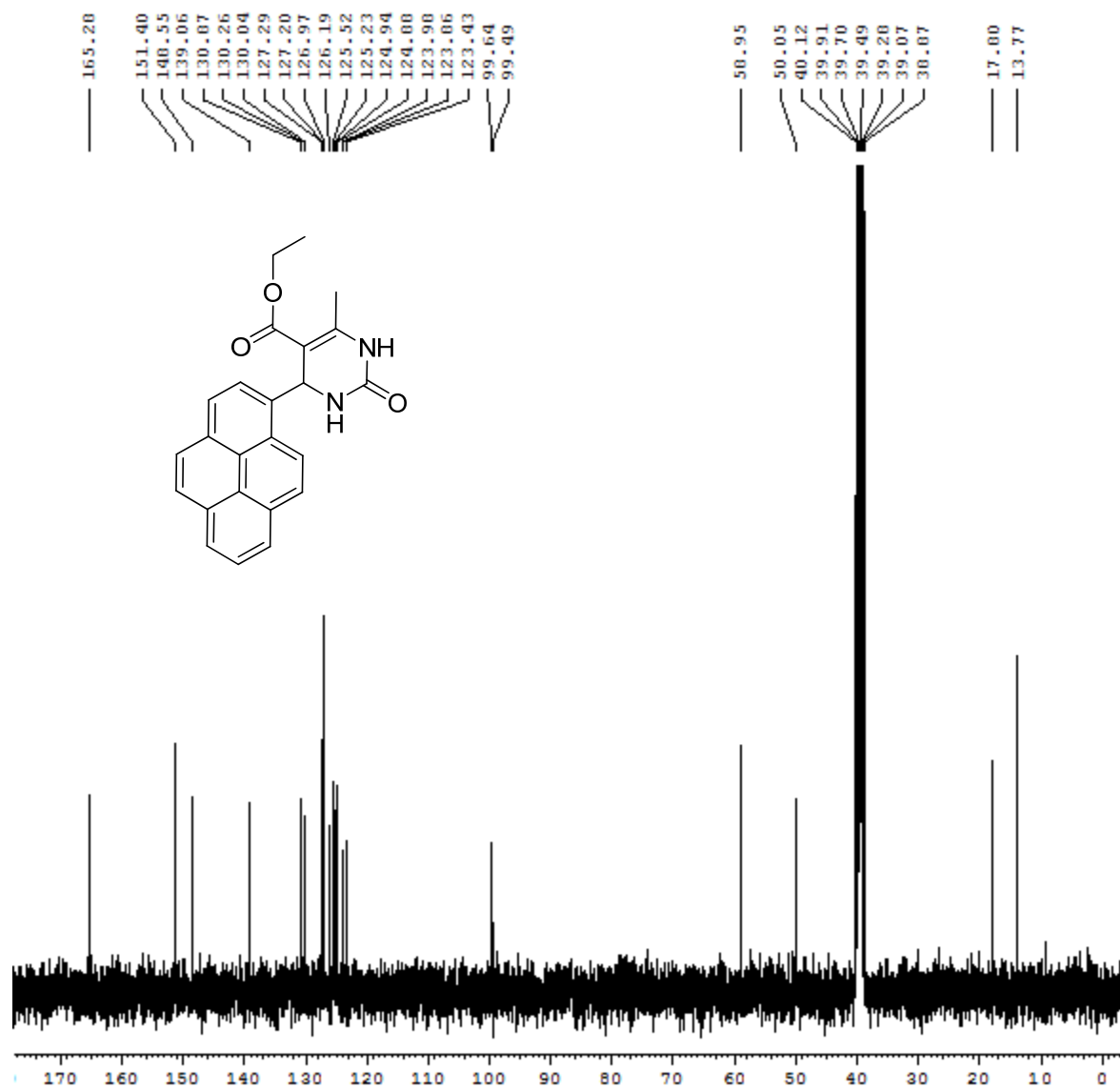


Figure S6. ^{13}C NMR spectrum of Sensor2.

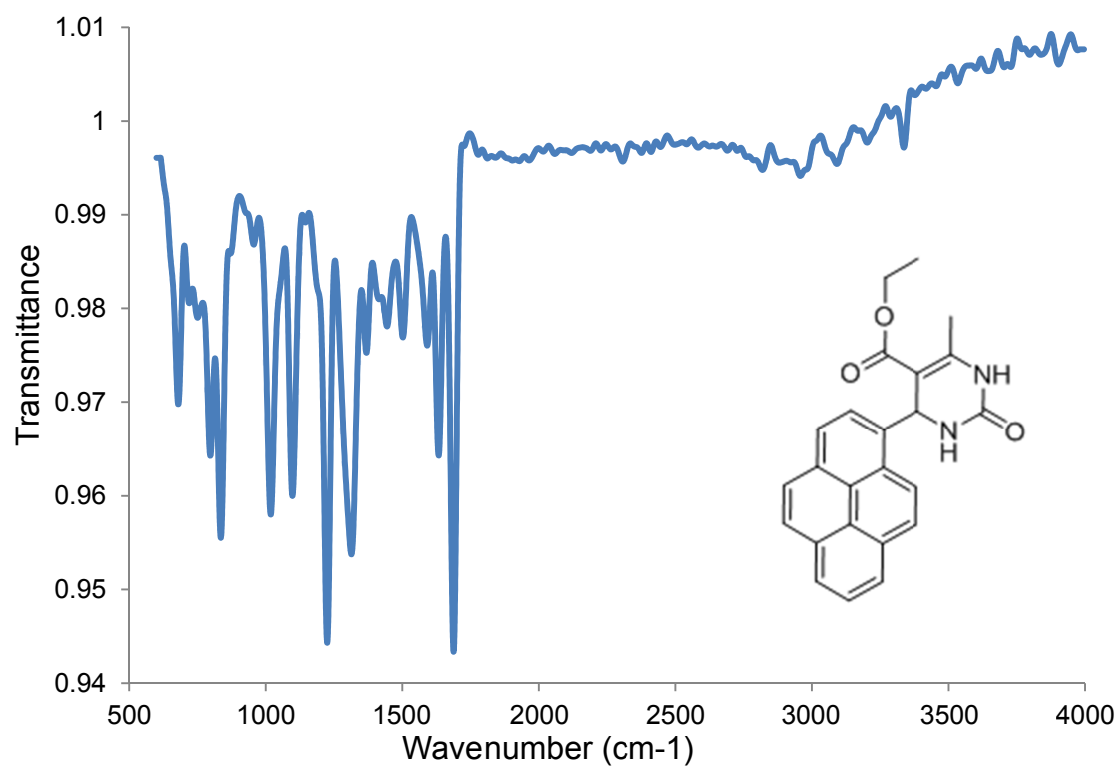


Figure S7. IR spectrum of Sensor 2.

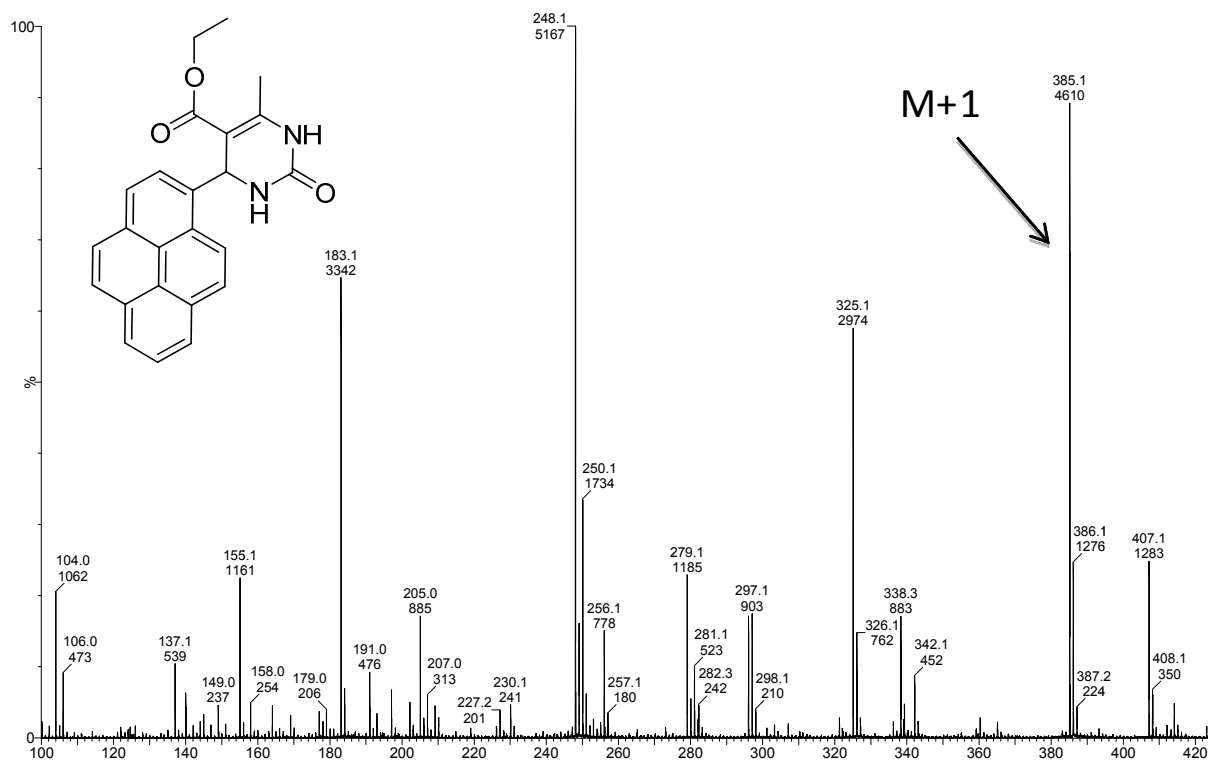


Figure S8. Mass spectrum of Sensor 2.

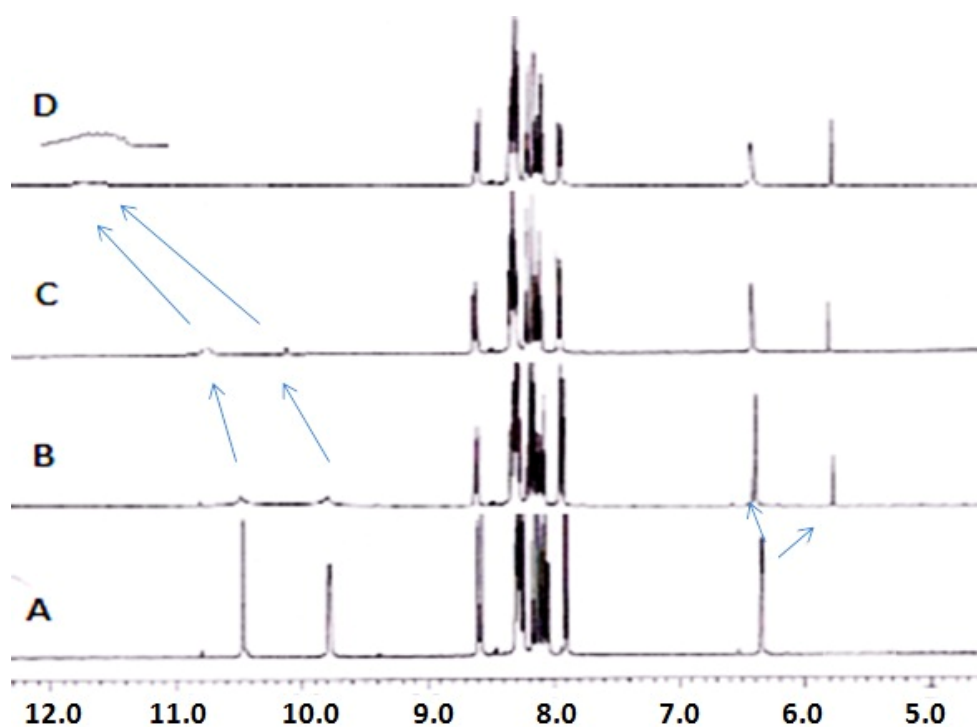


Figure S9. Stacked partial ¹H NMR spectra of: (A) Sensor 1 and (B-D) upon successive addition of Hg²⁺ to the solution of Sensor 1.

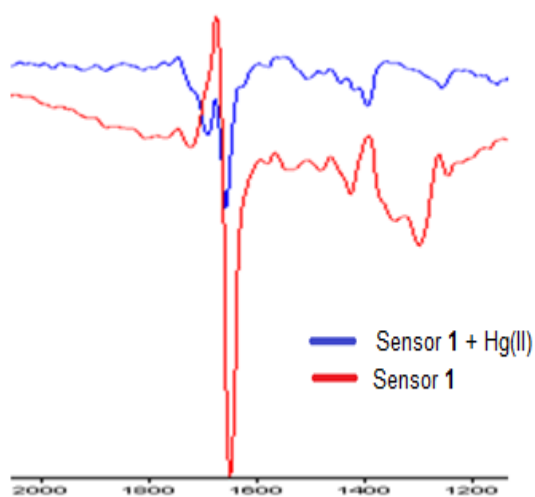


Figure S10. Stacked partial IR spectra of Sensor 1 and 1 + Hg²⁺.

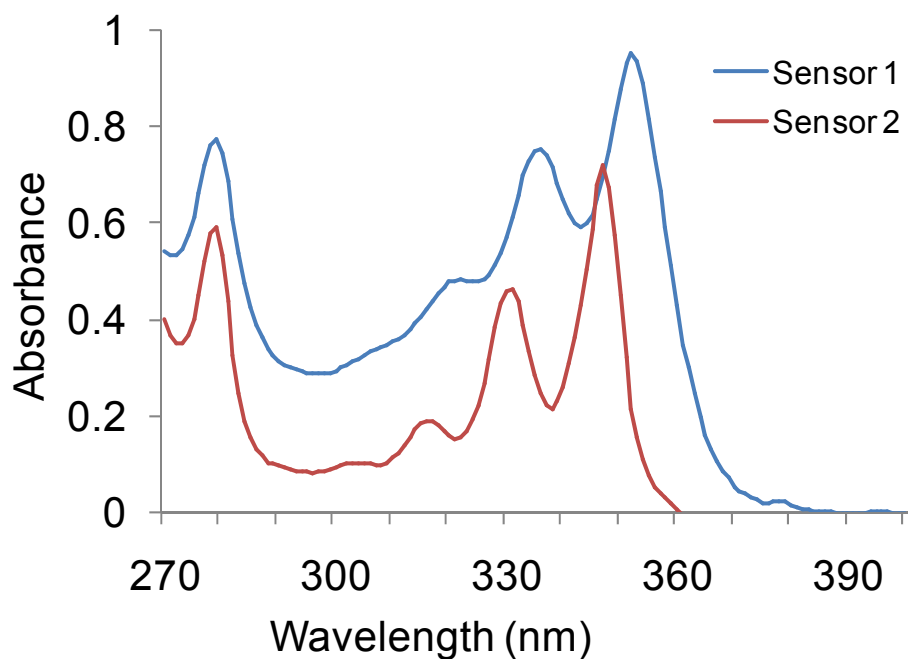


Figure S11. UV-Vis absorption spectra of 1-2 (10 μ M) in DMF/H₂O (7/3; v/v) solvent system.

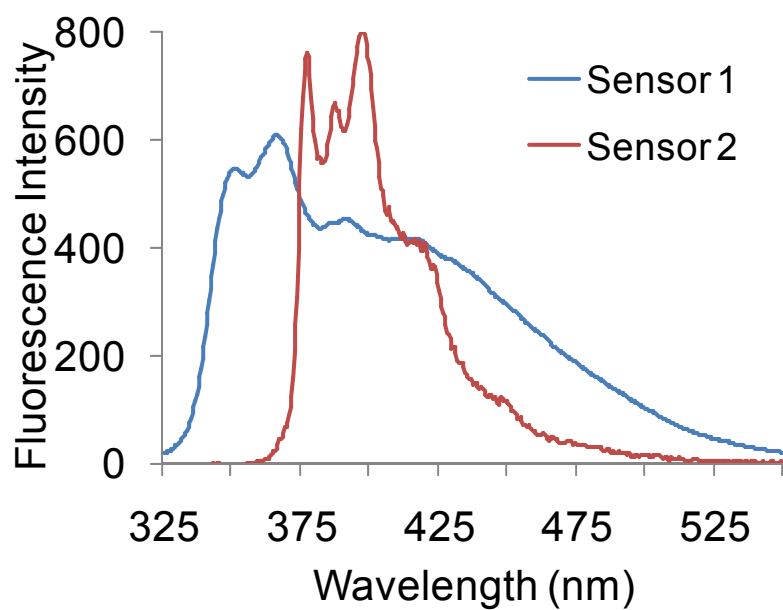


Figure S12. Fluorescence spectra of 1-2 (10 μ M) in DMF/H₂O (7/3; v/v) solvent system (λ_{ex} =338 nm).

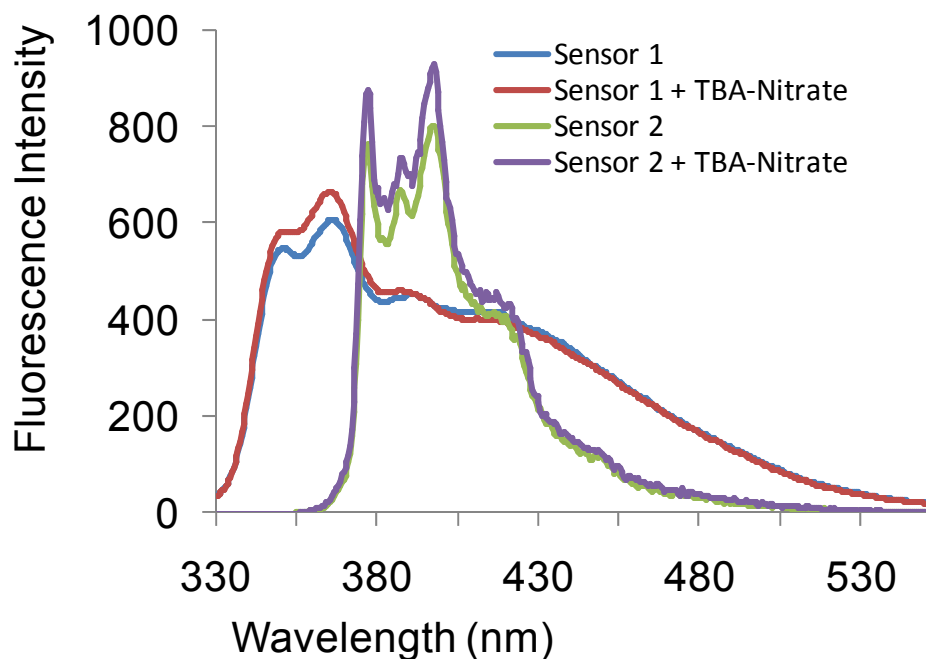


Figure S13. Salt perturbation studies of **1** recorded with 10 μM concentration of sensor in DMF/H₂O (7:3, v/v) solvent system with the respective fluorescence spectrum recorded upon addition of 100 equiv. of tetrabutylammonium nitrate under the same concentration of sensor and solvent system.

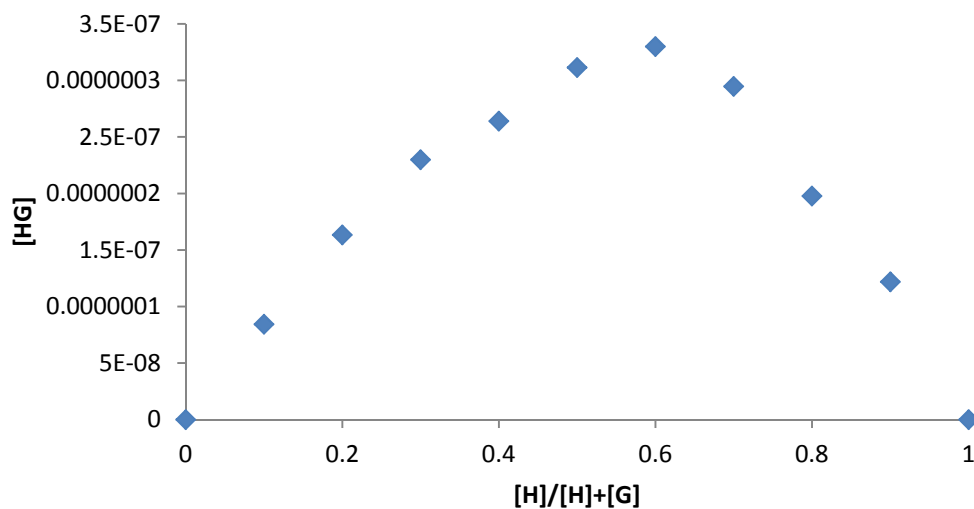


Figure S14. Job's plot between sensor **1** and Hg(II). The concentration of [HG] was calculated by the equation $[\text{HG}] = \Delta I/I_0 \times [\text{H}]$.

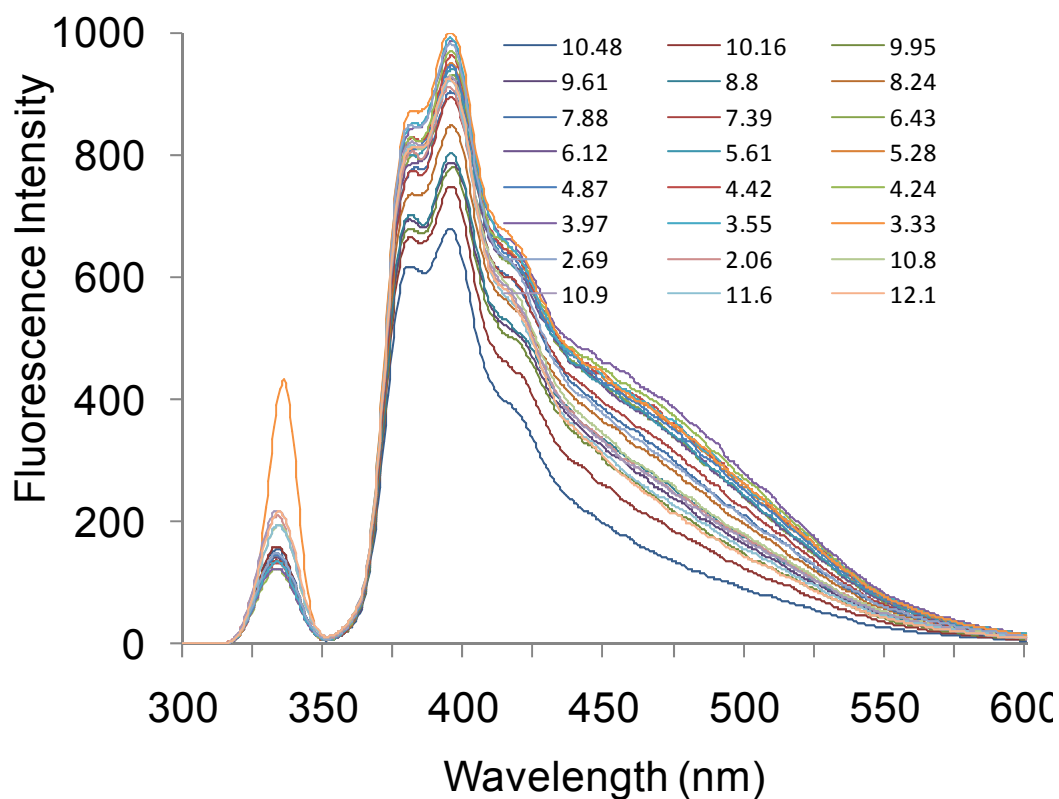


Figure S15. pH titration of Sensor1 ($10 \mu\text{M}$) in DMF/ H_2O (1/9; v/v) solvent system ($\lambda_{\text{ex}}=338 \text{ nm}$).

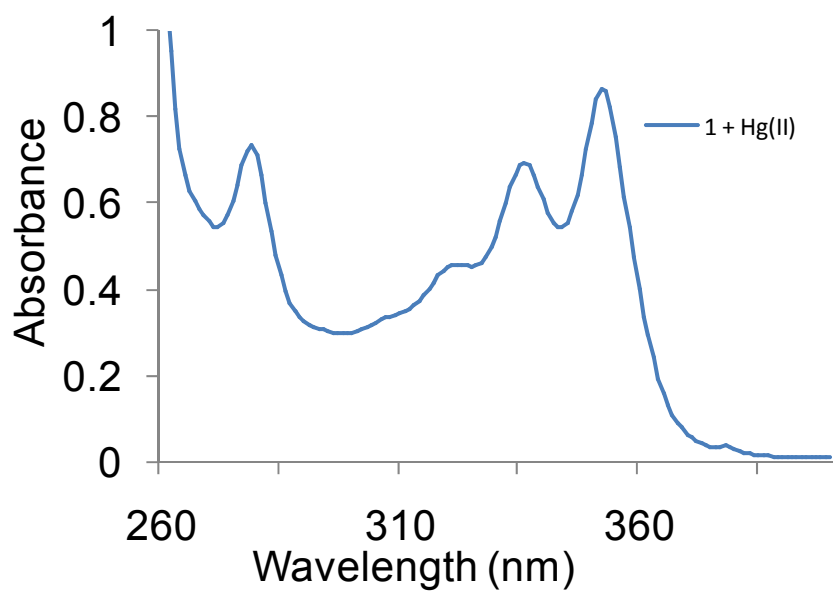


Figure S16. UV-Vis absorption spectra of $(1)_2 \cdot \text{Hg}^{2+}$ ($2.5 \mu\text{M}$) in THF/ H_2O (4:1, v/v) solvent system.

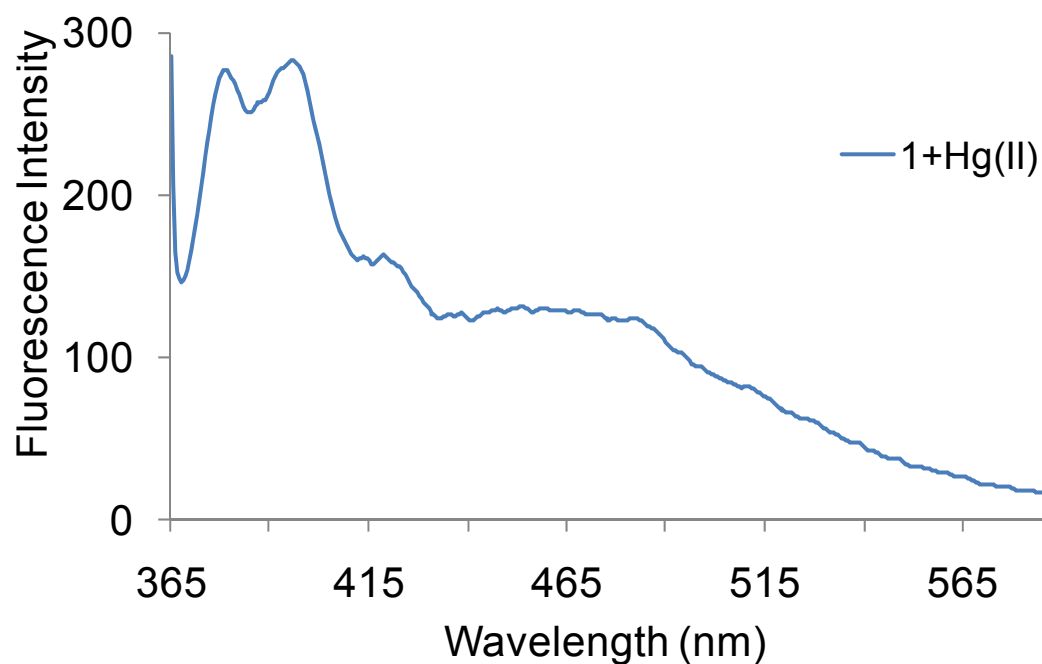


Figure S17. Fluorescence spectrum of $(\mathbf{1})_2\cdot\text{Hg}^{2+}$ ($2.5 \mu\text{M}$) in THF/ H_2O (4:1, v/v) solvent system ($\lambda_{\text{ex}}=338 \text{ nm}$).

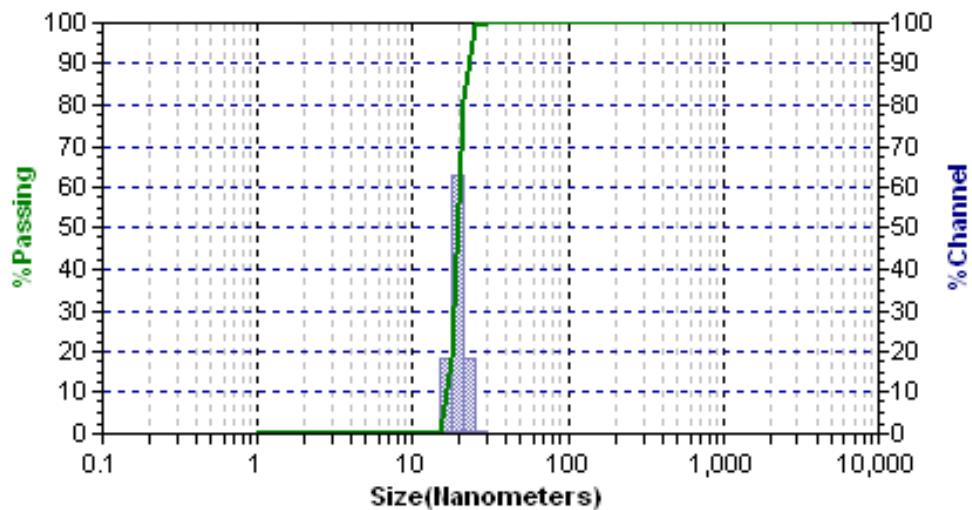


Figure S18. Size distribution of complex $(\mathbf{1})_2\cdot\text{Hg}^{2+}$ in DMF/ H_2O (8:92, v/v) solvent system.